JOURNAL OF SOLID STATE CHEMISTRY **141,** 404–410 (1998)
ARTICLE NO. SC987961

Magnetic and Neutron Diffraction Study on Perovskites $La_{1-x}Sr_xCrO_3$

Keitaro Tezuka and Yukio Hinatsu

Division of Chemistry, Graduate School of Science, Hokkaido University, Sapporo 060-0810, Japan

and

Akio Nakamura, Toshiya Inami, Yutaka Shimojo, and Yukio Morii

Japan Atomic Energy Research Institute, Tokai-mura, Ibaraki 319-1195, Japan

Received March 2, 1998; in revised form July 1, 1998; accepted July 2, 1998

Magnetic properties of perovskite-type compounds $La_{1-x}Sr_xCrO_3$ ($x = 0$, 0.05, 0.10, 0.15, 0.20, and 0.25) have been reported. Their DC magnetic susceptibilities were measured from 4.5 K to 320 K. All these compounds showed an antiferromagnetic transition and their Néel temperatures decreased linearly from 286 K for $LaCrO_3$ with increasing Sr substitution. Below the Néel temperatures, other two magnetic transitions were furthermore observed for almost all the compounds. Below the Néel temperatures, all the compounds except $LaCrO_3$ showed magnetic hysteresis. The initial magnetization curve indicates the existence of the metamagnetic property below 20 K. Powder neutron measurements were performed at room temperature, 250 K and 50 K for $La_{0.85}Sr_{0.15}CrO_3$. It was found that the crystal phase and magnetic transition occurred between 50 K and 250 K. The crystal structure at 250 K is rhombohedral with space group $R\bar{3}c$, and it transforms to an orthorhombic structure with space group *Pnma* at 50 K. The magnetic structures at 50 K and at 250 K are both the *G*-type. The direction of magnetic moments is directed to [111] of the rhombohedral unit cell at 250 K and changes to be parallel to the *z*-axis of the orthorhombic unit cell (*Pnma*) at 50 K.

INTRODUCTION

Lanthanum chromate $LaCrO_3$ is a perovskite-type compound. It is orthorhombic at room temperature, i.e., it has a so-called $GdFeO_3$-type structure with space group *Pnma* (No. 62) (1). At *ca.* 540 K, $LaCrO_3$ shows an orthorhombic-to-rhombohedral transition (2, 3). The rhombohedral phase has a $LaAlO_3$-type structure with space group $R\bar{3}c$ (No. 167) (4). The oxidation state of chromium in this $LaCrO_3$ is trivalent. Its electronic structure is $[Ar]3d^3$; $LaCrO_3$ is paramagnetic. This compound shows an antiferromagnetic ordering below 282 K (5).

Strontium-substituted $La_{1-x}Sr_xCrO_3$ has recently received much interest as an electrode material or interconnector for fuel cells, heating elements for high-temperature furnaces, etc., because of its high electric conductivity at high temperatures and heat-resistance (6–10). Although much research on the thermodynamics, conductivity, and sinterability (11) of these compounds has been reported, little is known of their chemical properties at low temperatures. In this study, we prepared solid solutions $La_{1-x}Sr_xCrO_3$ ($x = 0.05$, 0.10, 0.15, 0.20, and 0.25) and measured their DC magnetic susceptibilities to clarify the magnetic behavior of $3d$ electrons of chromium ions in this system. Furthermore, in addition to the X-ray diffraction measurements, powder neutron diffraction measurements have been performed for $La_{0.85}Sr_{0.15}CrO_3$ at low temperatures to elucidate its magnetic structure.

EXPERIMENTAL

A specimen $LaCrO_3$ was prepared by the standard solid state reaction. The starting materials were La_2O_3 and Cr_2O_3. (Because of its high hygroscopicity, La_2O_3 was heated in air at 1073 K for 8 h before use.) They were ground in an agate mortar, pressed into pellets, and fired in air at 1223 K for 12 h. After cooling, they were reground and fired in air at 1723 K for 20 h twice. In a similar way, the specimens $La_{1-x}Sr_xCrO_3$ ($x = 0.05$, 0.10, 0.15, 0.20, and 0.25) were prepared by mixing the starting materials, La_2O_3, Cr_2O_3, and $SrCO_3$ and firing in air at 1723 K for 96 h. After cooling, regrinding the mixtures and refiring them in a flow of oxygen gas at 1723 K for 14 h were repeated twice.

Powder X-ray diffraction patterns were measured with Cu-$K\alpha$ radiation on a RINT2000 diffractometer (Rigaku). The structures were refined with the Rietveld analysis method, using program Rietan (12).

Powder neutron diffraction pattern for $La_{0.85}Sr_{0.15}CrO_3$ were measured with a high resolution powder diffractometer (HRPD) in the JRR-3M reactor (Japan Atomic

0022-4596/98 $25.00

TABLE 1
Crystallographic Data for $La_{1-x}Sr_xCrO_3$ at Room Temperature from Powder X-ray Diffraction Profiles

Atom	Position	x	y	z	B/Å^2
$x = 0$ space group *Pnma* (No. 62)					
$a = 5.4813(1)$Å $b = 7.7611(1)$Å $c = 5.5181(1)$Å					
$R_{wp} = 10.34$ $R_I = 1.91$ $R_F = 1.57$					
La	4(*c*)	0.019(1)	0.25	0.006(1)	0.3
Cr	4(*b*)	0.0	0.0	0.5	0.3
O(1)	4(*c*)	0.494(3)	0.25	− 0.046(5)	0.3
O(2)	8(*d*)	0.271(4)	0.031(2)	− 0.281(3)	0.3
$x = 0.05$ space group *Pnma* (No. 62)					
$a = 5.4741(1)$Å $b = 7.7514(1)$Å $c = 5.5151(1)$Å					
$R_{wp} = 10.72$ $R_I = 3.41$ $R_F = 2.65$					
La, Sr	4(*c*)	0.017(1)	0.25	0.006(1)	0.3
Cr	4(*b*)	0.0	0.0	0.5	0.3
O(1)	4(*c*)	0.494(3)	0.25	− 0.037(5)	0.3
O(2)	8(*d*)	0.272(4)	0.033(2)	− 0.277(4)	0.3
$x = 0.15$ space group $R\bar{3}c$ (No. 167)					
$a = 5.4553(2)$Å $\alpha = 60.558(1)^\circ$					
$R_{wp} = 15.32$ $R_I = 2.91$ $R_F = 2.05$					
La, Sr	2(*a*)	0.25	0.25	0.25	0.3
Cr	2(*b*)	0.0	0.0	0.0	0.3
O	6(*e*)	− 0.301(5)	0.801(5)	0.25	0.3
$x = 0.25$ space group $R\bar{3}c$ (No. 167)					
$a = 5.4506(1)$Å $\alpha = 60.476(1)^\circ$					
$R_{wp} = 11.75$ $R_I = 2.40$ $R_F = 1.58$					
La, Sr	2(*a*)	0.25	0.25	0.25	0.3
Cr	2(*b*)	0.0	0.0	0.0	0.3
O	6(*e*)	− 0.204(4)	0.704(4)	0.25	0.3

Note. Isotropic thermal parameters (B) are fixed to be 0.3 Å^2.

Energy Research Institute), with Ge (331) monochrometor ($\lambda = 1.823$ Å). The collimators used were 6′–20′–6′, which were placed before and after the monochromator, and between the sample and each detector. The set of 64 detectors and collimators, which were placed every 2.5°, rotate around the sample. The measurements were made at 50 K, 250 K, and room temperature. Crystal and magnetic structure were also determined by the Rietveld technique.

DC magnetic susceptibilities were measured with a SQUID (Quantum Design, MPMS model) after zero field cooling (ZFC) and field cooling (FC) processes in the temperature range 4.5 K–320 K. The external magnetic field applied was 1000 G. The field dependence of the magnetization was measured at several temperatures by changing the magnetic field strength in the range between − 50000 G and 50000 G.

Differential thermal analysis (DTA) was performed for $LaCrO_3$ and $La_{0.95}Sr_{0.05}CrO_3$ with a 2000S equipment (Mac Science) in an oxygen flowing atmosphere in the temperature range between room temperature and 873 K.

RESULTS AND DISCUSSION

Crystal Structure

The compounds prepared in this study crystallize in single phases except for $La_{0.90}Sr_{0.10}CrO_3$. Their X-ray diffraction profiles were indexed with an orthorhombic unit cell, space group *Pnma* (No. 62) for ($x = 0.0$ and 0.05), and with a rhombohedral unit cell, space group $R\bar{3}c$ (No. 167) for ($x = 0.15$, 0.20, and 0.25). The data were analyzed by the Rietveld analysis method and the results are shown in Table 1. The crystal structures of some compounds are shown in Fig. 1. The compound $La_{0.90}Sr_{0.10}CrO_3$ is a two-phase composed of the orthorhombic phase and the rhombohedral phase.

It is often found that the crystal has a structure with higher symmetry at higher temperatures. For $LaCrO_3$ and $La_{0.95}Sr_{0.05}CrO_3$, the phase transitions should be observed by raising the temperature. We have found them through their DTA, and the orthorhombic-to-rhombohedral transition temperatures were determined to be 526 K and 413 K, respectively.

To discuss the stability of the perovskite-type compounds ABO_3, Goldshmit introduced the tolerance factor (t) defined by

$$t = \frac{r_A + r_O}{\sqrt{2}(r_B + r_O)},$$

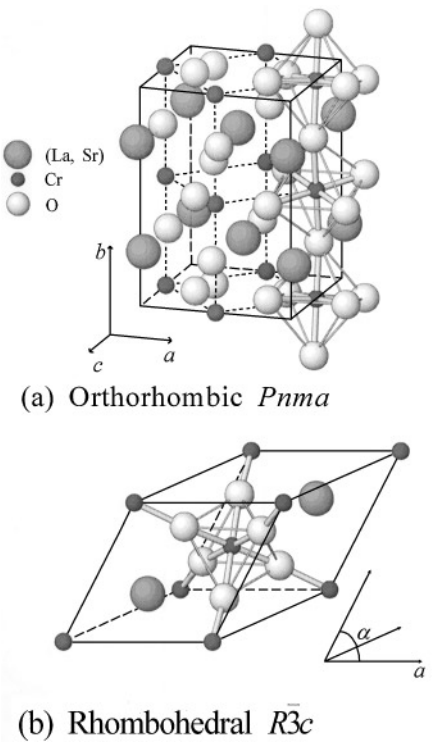

FIG. 1. Crystal structures of perovskite-type compounds: (a) an orthorhombic structure with space group *Pnma*; (b) a rhombohedral structure with space group $R\bar{3}c$.

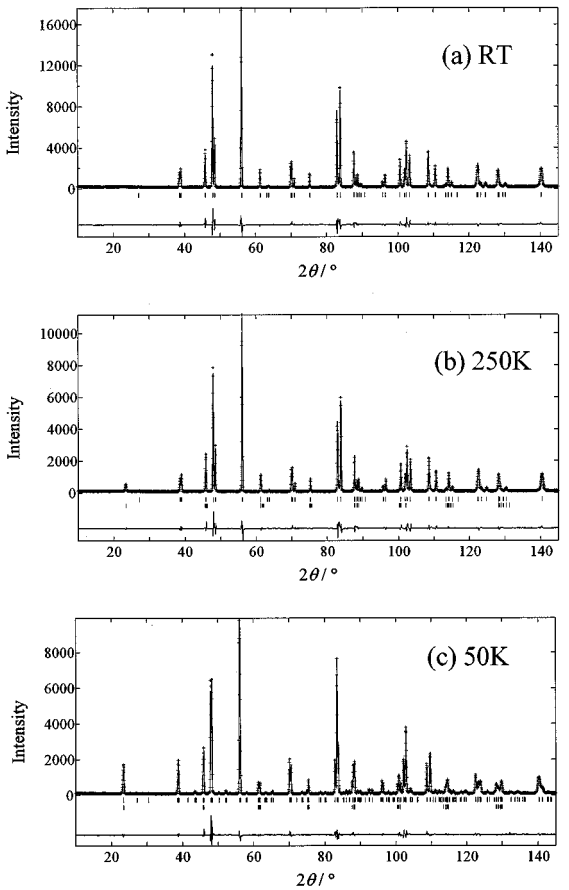

FIG. 2. Powder neutron diffraction pattern fitting for $La_{0.85}Sr_{0.15}CrO_3$. The calculated and observed patterns are shown on the top solid line and the cross markers, respectively. The vertical marks in the middle show positions calculated for Bragg reflections. The nuclear reflection positions are shown as upper vertical marks and the magnetic ones as lower ones. The lower trace is a plot of the difference between calculated and observed intensities: (a) at room temperature; (b) at 250 K; (c) at 50 K.

TABLE 2
Crystal and Magnetic Structure Data for $La_{0.85}Sr_{0.15}CrO_3$ from Powder Neutron Diffraction Profiles

Atom	Position	x	y	z	B/Å^2
room temperature space group $R\bar{3}c$ (No. 167)					
$a = 5.4587(2)$Å $\alpha = 60.592(2)^\circ$					
$R_{wp} = 10.27$ $R_I = 2.74$ $R_F = 1.45$					
magnetic moment: 0 μ_B					
La, Sr	2(*a*)	0.25	0.25	0.25	0.31
Cr	2(*b*)	0.0	0.0	0.0	0.30
O	6(*e*)	− 0.300(1)	0.800(1)	0.25	0.59
250 K space group $R\bar{3}c$ (No. 167)					
$a = 5.4556(2)$Å $\alpha = 60.611(3)^\circ$					
$R_{wp} = 11.35$ $R_I = 3.26$ $R_F = 1.68$					
magnetic moment: 1.27(12) μ_B					
direction of moment: [111] of rhombohedral unit cell					
La, Sr	2(*a*)	0.25	0.25	0.25	0.26
Cr	2(*b*)	0.0	0.0	0.0	0.24
O	6(*e*)	− 0.301(1)	0.801(1)	0.25	0.51
50 K space group *Pnma* (No. 62)					
$a = 5.4586(1)$Å $b = 7.7311(1)$Å $c = 5.5050(1)$Å					
$R_{wp} = 7.66$ $R_I = 1.84$ $R_F = 1.17$					
magnetic moment: 2.40(4) μ_B					
direction of moment: *c* axis					
La, Sr	4(*c*)	0.015(1)	0.25	− 0.003(1)	0.05
Cr	4(*b*)	0.0	0.0	0.5	0.08
O(1)	4(*c*)	0.496(1)	0.25	0.061(1)	0.13
O(2)	8(*d*)	0.232(1)	0.532(1)	0.232(1)	0.29

where r_A, r_B, and r_O are the radii of the A and B metal ions and oxygen ion, respectively. For tolerance factors less than unity, two types of distortion from the ideal cubic unit cell, the rhombohedral structure and the orthorhombic structure, commonly occur. For larger deviations from the ideal ionic radius ratios, the orthorhombic structure is observed. $LaCrO_3$ is the orthorhombic perovskite with $t = 0.969$. When the solid solutions $La_{1-x}Sr_xCrO_3$ are formed, some of the trivalent ions are oxidized to the tetravalent state with the substitution of Sr^{2+} for La^{3+}. With increasing Sr substitution, the average radius of the ions at the A sites of the perovskite (La^{3+}, Sr^{2+}) becomes larger and that of the ions at the B sites (Cr^{3+}, Cr^{4+}) becomes smaller. As a result of this, the tolerance factor becomes larger and the phase transition from an orthorhombic to a rhombohedral phase occurs at lower temperatures with increasing Sr substitution. If this transition temperature for $La_{1-x}Sr_xCrO_3$ decreases linearly with the Sr substitution, the transition temperature for $La_{0.90}Sr_{0.10}CrO_3$ is just around the room temperature. Therefore it is considered that preparation of a single-phase specimen for this composition ratio is difficult and two phases coexist at room temperature, as shown in this experiment.

Neutron diffraction measurements were also performed for the $La_{0.85}Sr_{0.15}CrO_3$ to determine the precise crystal structure and the magnetic structure at low temperature, and the results were analyzed by the Rietveld method. They are shown in Fig. 2 and Table 2. The result by the neutron diffraction measurements at room temperature agrees well with that by the X-ray diffraction measurements; i.e., this compound has a rhombohedral perovskite with space group $R\bar{3}c$. The crystal structure at 250 K has the same crystal structure as that at room temperature, although the cell volume at 250 K is smaller than that at room temperature. We have found that the crystal structure at 50 K has orthorhombic symmetry; i.e., the crystal phase transition from orthorhombic (*Pnma*) to rhombohedral ($R\bar{3}c$) occurred between 50 K and 250 K from the neutron measurements. The same phase transition has been found in $LaCrO_3$ and $La_{0.95}Sr_{0.05}CrO_3$ ($t = 0.969$ and $t = 0.972$, respectively) from our DTA measurements. Compared with the tolerance factors for these samples, the value for $La_{0.85}Sr_{0.15}CrO_3$

($t = 0.977$) is larger, and the crystal phase transition temperature for $La_{0.85}Sr_{0.15}CrO_3$ should be lower, which is consistent with this experimental result.

Magnetic Property

A. Magnetic susceptibility. Temperature dependence of the magnetic susceptibilities for the samples $La_{1-x}Sr_xCrO_3$ prepared in this study is shown in Fig. 3a. It is found that the behaviour of magnetic susceptibility against temperature under zero field cooling conditions is strongly affected by the substitution of Sr for La.

Compared with the case of $LaCrO_3$ (Fig. 3b), dramatic differences between ZFC and FC were observed below Néel temperatures for all the solid solutions, some of which are shown in Fig. 3c ($La_{0.95}Sr_{0.05}CrO_3$) and Fig. 3d ($La_{0.85}Sr_{0.15}CrO_3$).

The variation of the Néel temperatures for $La_{1-x}Sr_xCrO_3$ with Sr concentration is shown in Fig. 4. They decrease linearly with increasing Sr substitution for La. This is

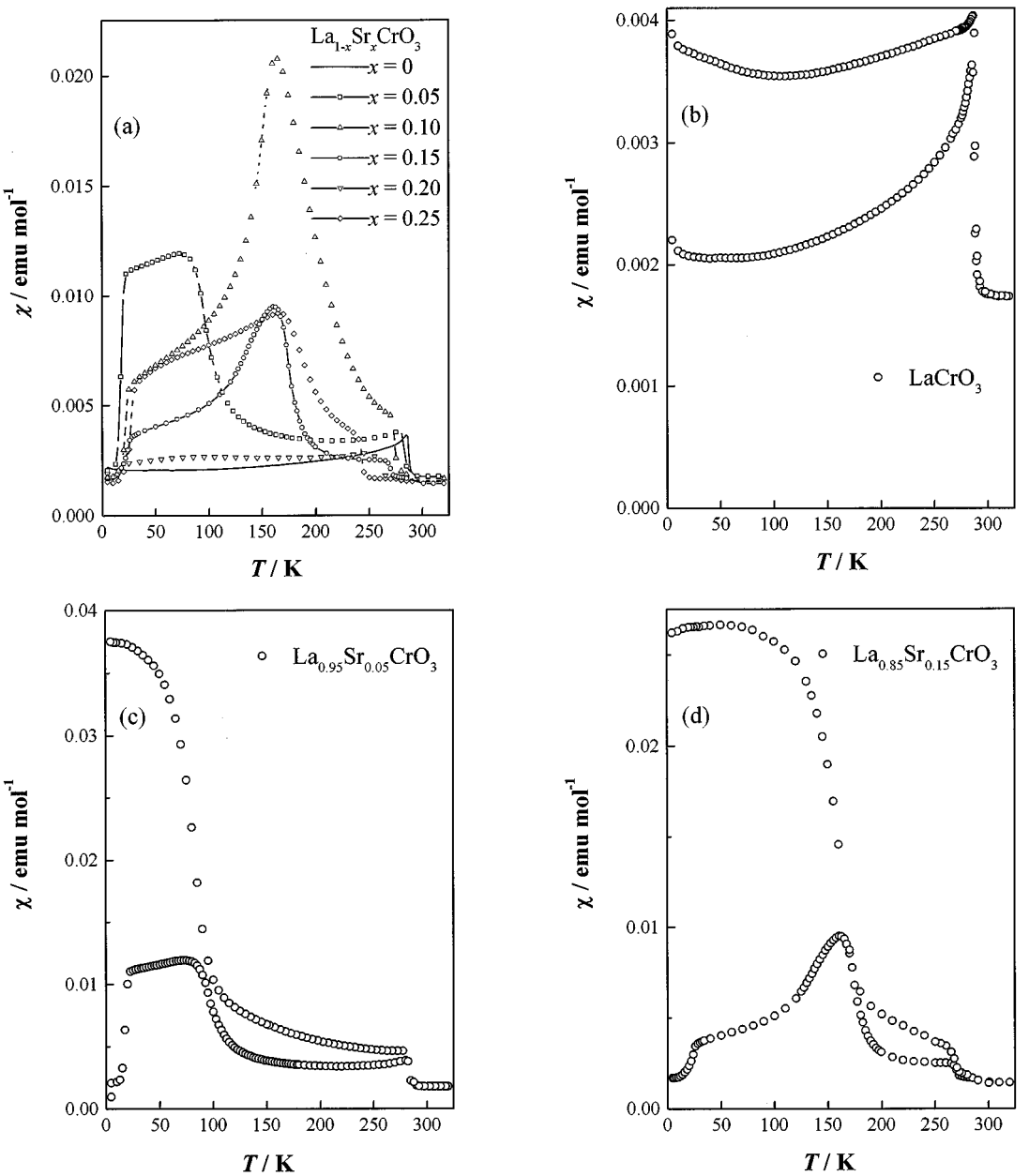

FIG. 3. DC magnetic susceptibilities for $La_{1-x}Sr_xCrO_3$ measured after zero field cooling (ZFC) and field cooling (FC): (a) ZFC for $La_{1-x}Sr_xCrO_3$; (b) ZFC (inferior curve) and FC (superior curve) for $LaCrO_3$; (c) ZFC and FC for $La_{0.95}Sr_{0.05}CrO_3$; (d) ZFC and FC for $La_{0.85}Sr_{0.15}CrO_3$.

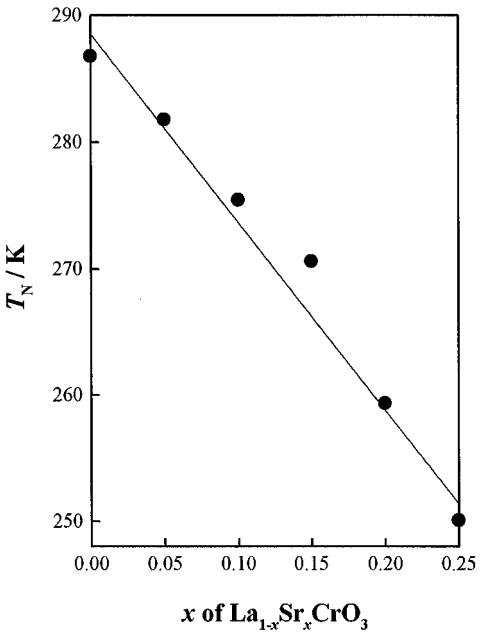

FIG. 4. Néel temperatures vs Sr substitution for $La_{1-x}Sr_xCrO_3$.

probably due to the fact that with increasing Sr concentration in the solid solution, the number of the Cr^{4+} ions ($3d^2$) increases and that of the Cr^{3+} ions ($3d^3$) decreases.

Below the Néel temperatures, the other two magnetic transitions were observed for almost all the $La_{1-x}Sr_xCrO_3$ (see Fig. 3a). One of the transitions occurs at the temperatures between 50 K and 250 K. At present, no systematic relation between the transition temperature and the Sr substitution for La has been found. The other magnetic transition is found at *ca.* 20 K. This transition temperature is independent of the Sr concentration of the compounds.

Below the Néel temperature, all the solid solutions prepared in this study show the magnetic hysteresis. Figure 5 shows the magnetization curve for $La_{0.85}Sr_{0.15}CrO_3$ measured at various temperatures. At 50 K and 5 K the magnetization depends greatly on the applied field. There exists a ferromagnetic component in the magnetic moment of chromium. It is calculated to be 0.05 μ_B/Cr from the magnetization curve. At 5 K, which temperature is lower than the second magnetic transition temperature (*ca.* 20 K), the metamagnetic behavior is found in the initial magnetization curve (see Fig. 5c).

B. Magnetic structure. In the powder neutron diffraction profiles measured at 250 K and 50 K (Figs. 2b and c), magnetic Bragg peaks are present.

First, we will consider the magnetic structure at 50 K. The crystal structure of $La_{0.85}Sr_{0.15}CrO_3$ at this temperature is orthorhombic with space group *Pnma* and the magnetic

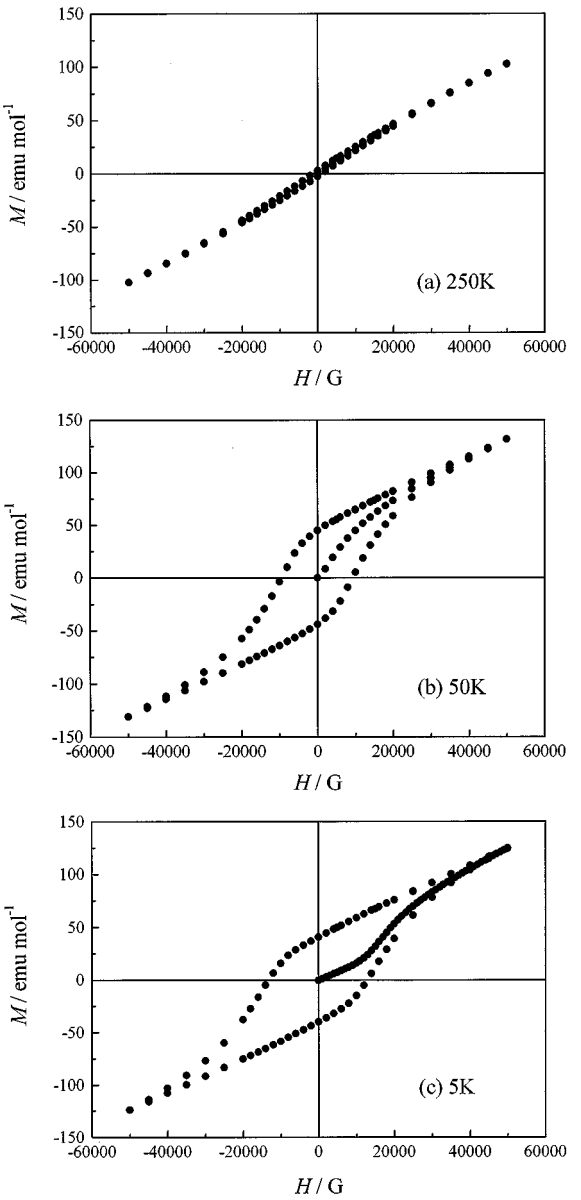

FIG. 5. Magnetic hysteresis curves for $La_{0.85}Sr_{0.15}CrO_3$: (a) at 250 K; (b) at 50 K; (c) at 5 K.

Bragg peaks can be indexed in the crystallographic unit cell with both $h + l$ and k odd.

In the orthorhombic space group *Pnma*, with Cr atoms in the 4*b* Wyckoff position, four magnetic sites are available in the unit cell, namely:

Position	x	y	z
Cr1	1/2	0	0
Cr2	1/2	1/2	0
Cr3	0	1/2	1/2
Cr4	0	0	1/2

with respective magnetic moments $\mathbf{S}_1$, $\mathbf{S}_2$, $\mathbf{S}_3$, and $\mathbf{S}_4$. Four types of magnetic arrangements are possible (13):

$$\mathbf{F} = \mathbf{S}_1 + \mathbf{S}_2 + \mathbf{S}_3 + \mathbf{S}_4$$

$$\mathbf{G} = \mathbf{S}_1 - \mathbf{S}_2 + \mathbf{S}_3 - \mathbf{S}_4$$

$$\mathbf{C} = \mathbf{S}_1 + \mathbf{S}_2 - \mathbf{S}_3 - \mathbf{S}_4$$

$$\mathbf{A} = \mathbf{S}_1 - \mathbf{S}_2 - \mathbf{S}_3 + \mathbf{S}_4.$$

It is known that for magnetic atoms in the 4*b* sites, some simple selection rules correspond to the *F*, *G*, *C*, and *A* types of magnetic moment arrangements as shown in Table 3. In the case of an *F*-type magnetic arrangement, the selection rule for the *F* type is equal to that of the nuclear diffraction at the 4*b* site; both the magnetic and nuclear Bragg reflections are found at the same diffraction angles.

From the selection rules in Table 3, the type of magnetic structure at 50 K is determined to be the *G* type. The direction of the magnetic moment was decided to be parallel to the *z*-axis, the G_z mode for $La_{0.85}Sr_{0.15}CrO_3$, from the Rietveld analysis (Table 2). This result contrasts with the result that the magnetic moment of $LaCrO_3$ is parallel to the *x*-axis, the G_x mode for $LaCrO_3$.

The G_z mode dominates for $La_{0.85}Sr_{0.15}CrO_3$ at 50 K. According to representation theory for *Pnma*, different sets of magnetic modes are possible, i.e., for the irreducible representation Γ_{1g} the G_x, C_y, and A_z modes; Γ_{2g} with C_x, G_y, and F_z; and Γ_{3g} with F_x, A_y, and C_z; and finally, Γ_{4g} with A_x, F_y, and G_z (13). The present G_z mode belongs to the irreducible representation Γ_{4g}. From magnetization measurements, we have found that there exists the ferromagnetic component in the magnetic moment of chromium (*F* type) at 50 K. However, the reflection intensity due to the magnetic diffraction is too small (the ferromagnetic moment is 0.05 μ_B/Cr from the hysteresis curve), compared with that due to the nuclear diffraction to estimate the component of the magnetic moment with *F* type from this powder neutron scattering pattern. It seems to be most possible that the ferromagnetic component of the magnetic moment (*F* type) is parallel to the *y*-axis because the mode F_y, transforming according to the same irreducible representation (Γ_{4g}) is considered.

TABLE 3
Selection Rule of Magnetic Bragg Peaks

Type	1 2 3 4[a]	$h+l$	k
F	+ + + +	Even	Even
G	+ − + −	Odd	Odd
C	+ + − −	Odd	Even
A	+ − − +	Even	Odd

[a] The numbers correspond to site number below.

Position	x	y	z
Cr1	1/2	0	0
Cr2	1/2	1/2	0
Cr3	0	1/2	1/2
Cr4	0	0	1/2

+ and − represent direction of magnetic moment and + is antiparallel to −.

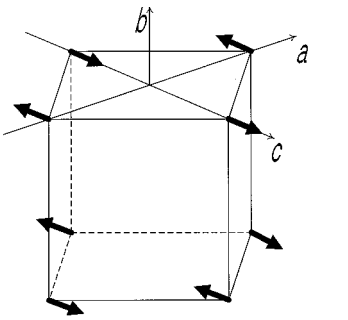

(a) 50K Orthorhombic (*Pnma*)

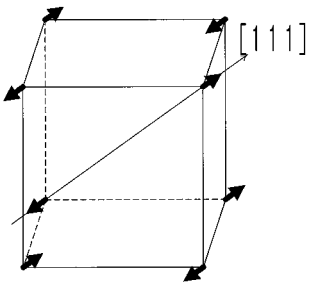

(b) 250K Rhombohedral ($R\bar{3}c$)

FIG. 6. Configuration of magnetic moments of Cr ions in pseudo-cubic cell for $La_{0.85}Sr_{0.15}CrO_3$: (a) at 50 K with an orthorhombic structure; (b) at 250 K with a rhombohedral structure.

The magnetic structure at 250 K has been also determined to be the *G* type from the magnetic Bragg reflection and magnetic moment is directed to [1 1 1] of the rhombohedral unit cell because [1 1 1] reflection intensity was not observed in this neutron diffraction experiment (Table 2). Since little magnetic hysteresis is found at 250 K (Fig. 5), the ferromagnetic component in the magnetic moment is nearly zero. Figures 6a and b show the magnetic structures determined for $La_{0.85}Sr_{0.15}CrO_3$ at 50 K and 250 K, respectively, assuming the pseudo-cubic perovskite-type unit cell for simplicity.

ACKNOWLEDGMENT

The present work was supported by Grant-in-Aid for Scientific Research 09874127 from the Ministry of Education, Science and Culture, Japan.

REFERENCES

1. S. Geller, *Acta Crystallogr*. **10,** 243 (1957).
2. S. Geller and P. M. Raccah, *Phys. Rev. B* **2,** 1167 (1970).
3. J. S. Ruiz, A. Anthony, and M. Foex, *Compt. Rend.* **264,** 1271 (1967).
4. C. P. Khattak and D. E. Cox, Argonne Natl. Lab. Report ANL, ANL-77-21, Conf. High Temp. Sci. Open-Cycle Coal-Fired MHD Syst., **160** (1977).
5. J. Faber Jr., M. H. Mueller, W. L. Procarione, A. T. Aldred, H. W. Knott, and H. U. Anderson, Argonne Natl. Lab. Report ANL, ANL-77-21, Conf. High Temp. Sci. Open-Cycle Coal-Fired MHD Syst., **154** (1977).
6. D. B. Meadowcroft, *Br. J. Appl. Phys.* **2,** 1225 (1969).
7. W. Baugal, W. Kunn, H. Kleischmager, and F. J. Rohr, *J. Powder Sources* **1,** 203 (1976/77).
8. W. Feduska and A. O. Isenberg, *J. Powder Sources* **10,** 89 (1983).
9. B. K. Flandermayer, J. T. Dusek, P. E. Blackburn, D. W. Dees, C. C. McPheeters, and R. B. Poepel, *in* "Abstracts from Fuel Cell Seminar, Tucson, AZ, 1986," p. 68. Courtesy Associated Inc., Washington, DC, 1986.
10. W. Shafer and R. Schmidberger, *in* "High Tech Ceramics" (P. Vincentini, Ed.). Elsevier, Amsterdam, 1987.
11. L. Groupp and H. U. Anderson, *J. Am. Chem. Soc.* **59,** 449 (1976).
12. F. Izumi, "The Rietveld Method" (R. A. Young, Ed.), Chap. 13. Oxford Univ. Press, Oxford, 1993.
13. E. F. Bertaut, *Acta Crystallogr. Sect. A* **24,** 217 (1968).